THE JOURNAL OF PHYSICAL CHEMISTRY Letters

Letter

Cite This: J. Phys. Chem. Lett. 2018, 9, 1944−1950

pubs.acs.org/JPCL

Interaction Enthalpy of Side Chain and Backbone Amides in Polyglutamine Solution Monomers and Fibrils

David Punihaole,[†] Ryan S. Jakubek,[‡] Riley J. Workman,[¶] and Sanford A. Asher*[,‡]

[†]Department of Chemistry, University of Minnesota, Minneapolis, Minnesota 55455, United States

[‡]Department of Chemistry, University of Pittsburgh, Pittsburgh, Pennsylvania 15260, United States

[¶]Department of Chemistry and Biochemistry, Center for Computational Sciences, Duquesne University, Pittsburgh, Pennsylvania 15282, United States

Supporting Information

ABSTRACT: We determined an empirical correlation that relates the amide I vibrational band frequencies of the glutamine (Q) side chain to the strength of hydrogen bonding, van der Waals, and Lewis acid−base interactions of its primary amide carbonyl. We used this correlation to determine the Q side chain carbonyl interaction enthalpy (ΔH_{int}) in monomeric and amyloid-like fibril conformations of $D_2Q_{10}K_2$ (Q10). We independently verified these ΔH_{int} values through molecular dynamics simulations that showed excellent agreement with experiments. We found that side chain−side chain and side chain−peptide backbone interactions in fibrils and monomers are more enthalpically favorable than are Q side chain−water interactions. Q10 fibrils also showed a more favorable ΔH_{int} for side chain−side chain interactions compared to backbone−backbone interactions. This work experimentally demonstrates that interamide side chain interactions are important in the formation and stabilization of polyQ fibrils.

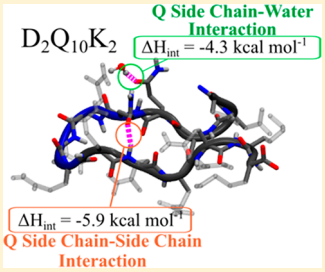

Ten neurodegenerative diseases, including Huntington's, are linked to mutational expansions of polyglutamine (polyQ) repeats in proteins.[1] The increase in polyQ repeats greatly enhances misfolding and aggregation of affected proteins. Although the exact mechanism of neurotoxicity is still heavily debated, the pathological hallmark of all of these diseases is the formation of neuronal aggregates composed of β-sheet-rich amyloid-like fibrils.[2−4] Given their potential role in neurotoxicity, there is great interest in understanding polyQ fibril formation, as well as developing therapeutic strategies to inhibit aggregation.

PolyQ peptides contain both primary amides from their glutamine (Q) side chains and secondary amides from their backbone peptide bonds. Despite the hydrophilic nature of the Q side chain, experimental studies indicate that polyQ peptides with pathologically relevant repeat lengths adopt structurally disordered collapsed conformations, which suggests that water is acting as a poor solvent.[5−10] These findings are also supported by computational studies,[11−14] which suggest that polyQ peptides are largely disordered due to the multiplicity of different hydrogen bonding interactions possible between side chain and backbone amides. Other computational studies suggest that interamide hydrogen bonds between side chains contribute most significantly to the structural stability of polyQ amyloid-like fibrils.[15]

These and other studies[1,16] underscore the crucial role that Q side chain hydrogen bonding interactions play in dictating the solution-state conformational behavior and the strong aggregation propensities of polyQ peptides. Surprisingly, however, no experimental studies have quantified the relative energetic favorability of side chain versus backbone amide hydrogen bonding interactions in polyQ peptides. Thus, developing new experimental tools that can quantify the relative energies of different side chain and backbone hydrogen bonding interactions is important to formulating a more complete, molecular-level understanding of polyQ fibril formation mechanisms.

Infrared and Raman spectroscopies can specifically probe interactions between different molecular species. One approach is to correlate the solvatochromatic frequency shifts of specific vibrational bands in solvents of different polarities to variations in interaction energies and hydrogen bonding strengths,[17] as first shown by Badger and Bauer.[18] Recent work by the Boxer group[19,20] and others,[21,22] however, has shown that the solvatochromatic shifts of many probes can often, but not always, be attributed to the vibrational Stark effect. Consequently, frequency shifts due to the vibrational Stark effect can be used to determine the local electric fields felt by the probes.

Using UV Resonance Raman (UVRR) spectroscopy, we previously showed that vibrational modes localized on the amide groups of Q's side chains are sensitive to their local structure,[23] hydrogen bonding, and dielectric environments.[24] For example, the amide I band of primary amides (denoted as AmI^P) sensitively probes the local hydrogen bonding of the Q side chain carbonyl group. The carbonyl stretching AmI^P band frequency and Raman cross section dramatically decrease in water relative to acetonitrile. Both of these spectral trends can

Received: February 1, 2018
Accepted: March 23, 2018
Published: March 23, 2018

DOI: 10.1021/acs.jpclett.8b00348
J. Phys. Chem. Lett. 2018, 9, 1944−1950

be rationalized by the fact that, compared to acetonitrile, water stabilizes the primary amide ground-state $^{-}O-C{=}NH_2^{+}$ resonance structure compared to the $O{=}C-NH_2$ resonance structure.[24]

The well-studied amide I bands of secondary amides (denoted as AmI^S) similarly show sensitivities to the solvation and local hydrogen bonding of the peptide bond backbone carbonyl groups.[25−29] Wang et al.[27] previously showed that the AmI^S frequency is linearly dependent on the solvent's acceptor number (AN), which is a measure of the strength of the solvent's hydrogen bonding, Lewis acid, and van der Waals interactions with solutes.[30] Using the AmI^S frequency−AN correlation, Wang et al. showed that the AmI^S frequency can be used to estimate the change in enthalpy due to these interactions (ΔH_{int}) for the secondary amide peptide bond carbonyl groups relative to that of these carbonyl groups in vacuum.

Inspired by Wang et al.'s[27] work, we investigated whether the AmI^P frequency could be used to determine the ΔH_{int} of the primary amide carbonyl groups with their chemical environments. We initially focused on the small primary amide model compound formamide because its ΔH_{int} values in various solvents are known.[31] We used the formamide solvent dependence of the AmI^P frequencies measured by Cutmore and Hallam[32] and the AmI^P frequency of formamide in water by Eaton et al.[33] to determine the frequency dependence on the solvent AN and donor number (DN).

Figure 1a shows the formamide AmI^P frequency dependence on the solvent AN and DN. There is a robust linear correlation

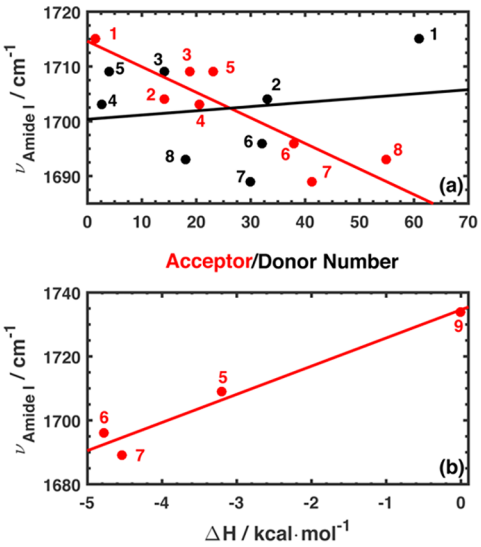

Figure 1. AmI^P frequency dependence of formamide on the (a) solvent AN, solvent DN, and (b) interaction enthalpy. The number labels in the figure correspond to the following solvents: (1) triethylamine; (2) pyridine; (3) acetonitrile; (4) nitromethane; (5) chloroform; (6) ethanol; (7) methanol; (8) H_2O; (9) vapor phase. The frequency dependence of formamide on the different solvents was obtained from data of Cutmore and Hallam[32] and Eaton et al.[33]

between the AmI^P frequency and solvent AN. The least-squares linear fit obtained from the AmI^P frequency dependence on the solvent AN is:

$$AmI^P = b + m(AN) = 1715\ cm^{-1} + (-0.50\ cm^{-1}\ acc\#^{-1})(AN) \quad (1)$$

where b = 1715 cm^{-1} and m = −0.50 cm^{-1} $acc\#^{-1}$ for formamide.

The donor number is a measure of a solvent's hydrogen bond accepting strength and Lewis basicity, which do not affect solvent−amide carbonyl group interactions.[27] Therefore, as expected, there is no correlation between the AmI^P frequency and solvent DN.

We also examined the AmI^P frequency dependence on the ΔH_{int} between the formamide carbonyl and different solvents using previously reported thermodynamic data.[31] For example, the ΔH_{int} values for the formamide carbonyl group in hydrogen bonding donor solvents such as ethanol, methanol, and chloroform and in the vapor phase are −4.8, −4.5, −3.2, and 0 kcal mol^{-1}, respectively (Figure 1b), indicating that the AmI^P frequency linearly depends on ΔH_{int}, with m' = 8.8 cm^{-1} $kcal^{-1}$ mol and b' = 1735 cm^{-1} for formamide:

$$AmI^P = b' + m'(\Delta H_{int}) = 1735\ cm^{-1} + (8.8\ cm^{-1}\ kcal^{-1}\ mol)(\Delta H_{int}) \quad (2)$$

Numerous studies have characterized the dependence of the AmI^P frequencies on the solvent AN. Unfortunately, few studies have characterized the dependence of the AmI^P frequencies on ΔH_{int}. Fortunately, we can convert the AmI^P frequency dependence upon AN to its dependence upon ΔH_{int} by relating eqs 1 and 2, as prescribed by Wang et al.[27]

First, the AN value of the solvent "vacuum" is determined by equating eqs 1 and 2 for formamide in vacuum. We calculate that AN = −40 (acc#) for the "vacuum solvent". Thus, the eq 2 intercept is $b' = b + m$ (−40 (acc#)). The AN of vacuum, as well as that of other solvents, is independent of the solute present. Thus, the intercept of eq 2 can be determined for any primary amide as long as the AmI^P frequency dependence on AN is known.

The AmI^P frequency is linearly proportional to both AN and ΔH_{int}. Thus, we can calculate the conversion factor between AN and ΔH_{int} for formamide from the slopes of eqs 1 and 2:

$$m = \frac{-0.50\ cm^{-1}}{1\ acc\#} = m' = \frac{8.8\ cm^{-1}}{1\ kcal\ mol^{-1}}$$

$$(1\ acc\#^{-1}) = \frac{8.8\ cm^{-1}\ kcal^{-1}\ mol}{-0.50\ cm^{-1}} = -18\ kcal^{-1}\ mol \quad (3)$$

Assuming that the conversion factor is constant for all primary amide compounds, eq 2 can be written as follows:

$$AmI^P = b' + m'(\Delta H_{int}) = (b + m(-40\ acc\#)) + (-18\ kcal^{-1}\ mol(m(\Delta H_{int}))) \quad (4)$$

Using eq 4, we can estimate ΔH_{int} for any primary amide compound from its AmI^P frequency dependence on AN.

Because Q and polyQ peptides have very limited solubility in low AN solvents, we often utilize propanamide as an alternative compound to model the Q side chains.[23,24,34] We previously found, using UVRR spectroscopy, that the AmI^P frequency of propanamide ($CH_3CH_2CONH_2$) is 1669 cm^{-1} in water and 1692 cm^{-1} in acetonitrile.[24] Because the AN of water is 54.8 while that of acetonitrile is 18.9,[35] we can calculate the linear dependence of the propanamide AmI^P frequency on AN. We find that m = −0.64 cm^{-1} $(acc\#)^{-1}$ and b = 1704 cm^{-1} for propanamide. By substituting these values into eq 4, we derive eq 5, which can be used to estimate ΔH_{int} for propanamide:

DOI: 10.1021/acs.jpclett.8b00348
J. Phys. Chem. Lett. 2018, 9, 1944−1950

Table 1. Estimated ΔH_{int} Values for Q Side Chain Carbonyl Groups in Different Peptide Conformations

	AmI^P (cm^{-1})	expt. (kcal mol^{-1})	MD sim. (kcal mol^{-1})	H-bonding type[a]
Q amino acid	1679	−4.3	–	s.c.−w
PPII	1680	−4.2	−4.4	s.c.−w
β-strand	1660, 1679	−5.8, −4.3	−4.7, −4.4, −4.6	s.c.−p.b., s.c.−w, s.c.−s.c.
fibrils prepared from β-strand monomers	1659	−5.9	−6.2	s.c.−s.c.
fibrils prepared from PPII monomers	1665	−5.4	−6.2	s.c.−s.c.

[a]s.c.: side chain; p.b.: peptide backbone; w: water.

$$AmI^P(cm^{-1}) = 1730(cm^{-1}) + (12\ cm^{-1}\ kcal^{-1}\ mol)(\Delta H_{int}) \quad (5)$$

Because propanamide models the Q side chain, we can use eq 5 to estimate the ΔH_{int} of side chain carbonyl groups in monomeric Q and in the polyQ peptide $D_2Q_{10}K_2$ (Q10) in any environment. The ΔH_{int} of each system is measured with respect to the vapor phase, where ΔH_{int} is zero. In the case of monomeric Q in aqueous solution, where the side chain carbonyl groups are hydrogen bonded to water, the AmI^P band is located at 1679 cm^{-1}.[23] As shown in Table 1, this frequency corresponds to a ΔH_{int} of −4.3 kcal mol^{-1}.

We recently showed that Q10 adopts two stable monomeric conformations in aqueous solution.[34] One solution conformation is a polyproline II (PPII)-like structure, which can be prepared using a standard "disaggregation" protocol.[36] The side chain and peptide backbone amides of this PPII-like conformation are hydrogen bonded to water molecules. The other conformation is a collapsed β-strand-like conformation, which is simply prepared by dissolving the synthesized peptide in water. The side chains of the β-strand-like conformations are intramolecularly hydrogen bonded, as well as to solvating water molecules. Both PPII-like and collapsed β-strand-like Q10 conformations can be poised to aggregate into different amyloid-like fibril polymorphs when incubated in aqueous solutions at elevated temperatures for about 1 week. The cores of fibrils grown from both monomeric conformations are composed almost exclusively of antiparallel β-sheets, though slight structural differences between the two polymorphs are observed.[37] Both fibril polymorphs, however, form interamide side chain hydrogen bonds between neighboring strands within a given β-sheet.[37]

Our previous studies[34,37] examined the AmI^P frequencies of these Q10 fibrils, as well as of the PPII-like and β-strand-like solution monomers. Table 1 shows these frequencies and their corresponding estimated ΔH_{int} values determined using eq 5. As expected, the ΔH_{int} of side chain carbonyl−water interactions in PPII-like and β-strand-like monomers are identical to those of monomeric glutamine in aqueous solution. In contrast, the ΔH_{int} of side chain carbonyl−peptide interactions that occur in the β-strand-like monomers are −5.8 kcal mol^{-1}, a value similar to that estimated for side chain−side chain interactions in polyQ fibrils. For fibrils prepared from PPII-like monomers, we determine that the ΔH_{int} value of side chain−side chain interactions is −5.4 kcal mol^{-1}, while that prepared from β-strand-like monomers is found to be −5.9 kcal mol^{-1}. This result may suggest that fibrils prepared from the PPII monomer have weaker side chain−peptide interactions. However, the difference between ΔH_{int} values for fibrils grown from the two different monomer states is within the estimated error, as discussed in the Supporting Information.

In determining these ΔH_{int} values, we implicitly assume that there is no significant coupling between AmI^P oscillators. Strong coupling of neighboring oscillators would cause "excitonic" splitting of the AmI^P band frequency, which would complicate the determination of ΔH_{int}. In dilute solutions of amides, such as for monomeric glutamine in water, no coupling of the AmI^P vibrations can occur. In the case of Q10 PPII-like and β-strand-like peptide monomers, we expect that coupling will likely be weak, so that the impact of band splitting on the AmI^P frequency is essentially negligible.

In contrast, neighboring oscillator coupling could impact the AmI^P band of polyQ fibrils. In antiparallel β-sheet conformations, for example, the backbone AmI^S frequency is impacted by coupling with neighboring oscillators, which results in band splitting (vide infra). However, in the case of the AmI^P, we see no evidence of coupling between the neighboring oscillators of Q10 fibrils. Our previously reported UVRR AmI^P bands of Q10 fibrils are very narrow and consist of only single bands,[37] suggesting no excitonic splitting. This conclusion is further reinforced by the fact that the Raman AmI^P frequencies of Q10 fibrils are essentially the same as reported IR frequencies of fibrils prepared from similar polyQ peptides.[38,39] This fact precludes the possibility that we only observe "bright" (Raman-active) exciton modes of the AmI^P, but no "dark" (Raman-inactive) modes.

We sought to compare the ΔH_{int} of side chain−side chain and backbone−backbone hydrogen bonds in Q10 fibrils. To estimate the ΔH_{int} of backbone−backbone interactions, we used an equation derived by Wang et al.[27] for the AmI^S band. However, the fibril AmI^S bands are impacted by coupling. As a result, it was first necessary to determine the uncoupled AmI^S frequencies of Q10 fibrils prepared from PPII-like and β-strand-like monomer solutions.

The excitonic splitting pattern of the AmI^S band in antiparallel β-sheets is well understood. Given the approximate D_2 symmetry of antiparallel β-sheets, the AmI^S vibration is predicted to split into four vibrational states, the A, B_1, B_2, and B_3 modes, all of which are Raman-active. We curve fit the AmI^S bands of Q10 fibrils from our previously published data (Figure S1) and assigned the A, B_1, B_2, and B_3 modes using the work of Krimm and co-workers[40−42] as a guide. Our spectral analysis of Q10 fibrils prepared from β-strand-like monomer solutions indicates that the A mode is located at 1665 cm^{-1}, the B_1 mode is at 1695 cm^{-1}, the B_2 mode is at 1625 cm^{-1}, and the B_3 mode is at 1680 cm^{-1}.[37] In contrast, for fibrils prepared from PPII-like monomers, the AmI^S A, B_1, B_2, and B_3 modes are located at 1660, 1688, 1617, and 1675 cm^{-1}, respectively.[37]

To estimate the unperturbed AmI^S frequencies, we utilize the perturbation theory approach developed by Miyazawa,[43] where the observed frequencies of the AmI^S bands are given by:

$$AmI^S(\delta, \delta') = \nu_0 + \sum_{s,t} D_{s,t} \cos(s\delta) \cos(t\delta') \quad (6)$$

DOI: 10.1021/acs.jpclett.8b00348
J. Phys. Chem. Lett. 2018, 9, 1944−1950

where ν_0 is the unperturbed AmI^S frequency, and $D_{s,t}$ are the interaction constants between peptide backbone amides separated by s amide groups and t chains along the tth peptide chain. δ and δ' are the phase angles between adjacent AmI^S oscillators along a given peptide chain or between hydrogen bonded peptide backbone amides on neighboring chains.

Moore and Krimm[40−42] have shown that for an infinite size antiparallel β-sheet system (which is an appropriate limit for Q10 fibrils) eq 6 can be written as:

$$\mathrm{AmI}^S(\delta, \delta') = \nu_0 + D_{00} + D_{10}\cos(s\delta) + D_{01}\cos(t\delta') + D_{11}\cos(s\delta)\cos(t\delta') \quad (7)$$

For antiparallel β-sheets, the following set of equations can be written from eq 7 by assuming different combinations of 0 or π phase angles:

$$\mathrm{AmI}^S(0,0) = \nu_0 + D_{00} + D_{10} + D_{01} + D_{11}$$
$$\mathrm{AmI}^S(0,\pi) = \nu_0 + D_{00} + D_{10} - D_{01} - D_{11}$$
$$\mathrm{AmI}^S(\pi,0) = \nu_0 + D_{00} - D_{10} + D_{01} - D_{11}$$
$$\mathrm{AmI}^S(\pi,\pi) = \nu_0 + D_{00} - D_{10} - D_{01} + D_{11} \quad (8)$$

where AmI^S(0, 0) corresponds to the A mode, while AmI^S(0, π), AmI^S(π, 0), and AmI^S(π, π) correspond to the B_1, B_2, and B_3 modes, respectively. The unperturbed frequency of the AmI^S cannot be exactly determined in eq 7 because there are too many unknown coefficients to solve. However, we can estimate an effective unperturbed frequency by substituting ν_0 with:

$$\nu'_0 = \nu_0 + D_{00} \quad (9)$$

Thus, using the experimentally observed AmI^S A, B_1, B_2, and B_3 mode frequencies for Q10 fibrils prepared from β-strand-like (PPII-like) monomer solutions, we determine ν'_0 to be 1663 cm^{-1} (1660 cm^{-1}), D_{10} to be 6.3 cm^{-1} (7.5 cm^{-1}), D_{01} to be −21.3 cm^{-1} (−21.5 cm^{-1}), and D_{11} to be 13.8 cm^{-1} (14 cm^{-1}).

Our calculated ν'_0, D_{01}, D_{10}, and D_{11} constants match in sign and are close in value to those determined by Krimm and co-workers for polyalanine and polyglycine antiparallel β-sheets.[40−42] This gives us confidence that ν'_0 can be used to robustly estimate ΔH_{int} for interamide hydrogen bonds formed between peptide bonds in the core of polyQ fibrils.

To estimate ΔH_{int} from ν'_0, we used the following equation derived by Wang et al.[27] for *N*-acetyltrialanine methyl ester:

$$\mathrm{AmI}^S = 1699.3\ \mathrm{cm}^{-1} + (9.46\ \mathrm{mol\ cm}^{-1}\ \mathrm{kcal}^{-1})(\Delta H_{int}) \quad (10)$$

Using eq 10, we estimate that the ΔH_{int} of backbone−backbone interactions is −3.8 kcal mol^{-1} for fibrils prepared from both Q10 β-strand-like and PPII-like monomers. This interaction strength is similar to NMA−NMA hydrogen bonding strengths previously measured.[44−46]

The above ΔH_{int} values indicate that backbone−backbone interactions in Q10 fibrils are enthalpically less favorable than side chain−side chain hydrogen bonding interactions. It is possible that the difference in the ΔH_{int} values for interamide backbone versus side chain interactions results from our use of ν'_0 instead of ν_0 when calculating ΔH_{int}. Krimm and co-workers estimate that D_{00} is relatively small (roughly −5 cm^{-1}). Using a D_{00} value of −5 cm^{-1}, we roughly estimate that side chain−side chain interactions are still enthalpically more favorable (by ∼−1 kcal mol^{-1}) than backbone−backbone interactions.

In our previous work, we used metadynamics and molecular dynamics (MD) simulations, in conjunction with UVRR, to investigate the monomer solution-state and fibril structures of Q10.[34,37] Here, we use our previously simulated Q10 structures as initial coordinates to perform classical MD simulations on solution-state and fibril Q10 conformations. We use these simulations to independently calculate ΔH_{int} values of various backbone and side chains interactions and compare them to that obtained via UVRR.

Figure 2 shows the simulated PPII-like, β-strand-like, and fibril structures. For each structure, we determined the average

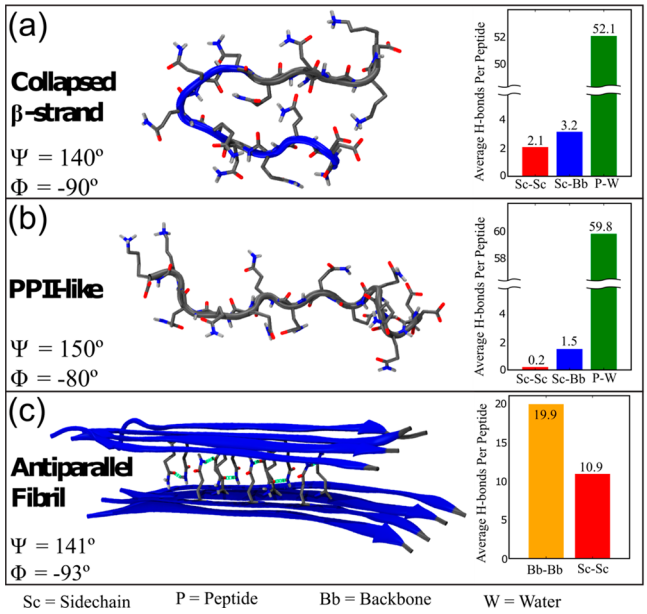

Figure 2. Structures and backbone Ramachandran angles of MD simulated Q10 structures in the (a) monomeric collapsed β-strand-like, (b) monomeric PPII-like, and (c) antiparallel fibril conformations. The bar graphs show the average number of various hydrogen bonding interactions per peptide residue.

number of interamide (e.g., side chain−side chain, side chain−backbone, and backbone−backbone) and amide−water hydrogen bonding interactions formed per peptide (Figure 2). We define a hydrogen bond as having a geometry such that the heavy atom donor to acceptor distance is <3.0 Å with a bond angle of 180° (±30).

The number of backbone−backbone hydrogen bonds is negligible for both the PPII-like and β-strand-like monomeric Q10 structures. For the monomeric PPII-like structure, we find that 94% of side chain amides are hydrogen bonded to water, 2% of side chains are hydrogen bonded to backbone amides, and 4% of side chains are hydrogen bonded to other side chains. For the β-strand-like structure, 66% of side chain amides are hydrogen bonded to water, 20% of side chains are hydrogen bonded to backbone amides, and 16% of side chains are hydrogen bonded to each other. In contrast, the Q10 antiparallel fibril structure's interior backbone and side chain amides are hydrogen bonded exclusively to other backbone and side chain amides.

From our MD simulations, we calculated average ΔH_{int} values for each simulated structure. We define ΔH_{int} as the sum of the Lennard-Jones ($\Delta E^{LJ}{}_{int}$) and Coulombic potential energy ($\Delta E^{elec}{}_{int}$) terms, where the Δ signifies the difference in energy of the carbonyl oxygen atoms with their interacting

DOI: 10.1021/acs.jpclett.8b00348
J. Phys. Chem. Lett. 2018, 9, 1944−1950

partner atoms in close proximity relative to being infinitely separated. Due to the negligible change in volume throughout the simulations, the ΔH_{int} can be accurately approximated as the change in the energy of interaction (ΔE_{int})

$$\Delta H_{int} \approx \Delta E_{int} = \Delta E_{int}^{elec} + \Delta E_{int}^{LJ} \quad (11)$$

When calculating ΔH_{int}, we define interacting groups as those with heavy atoms at distances of less than or equal to 5 Å. Thus, our calculated ΔH_{int} is not limited to strong hydrogen bonding interactions, which generally occur for heavy atom distances less than 3 Å. For the Q10 antiparallel β-sheet conformation (Figure 2c), the six innermost buried side chain and backbone amide groups were used to calculate the ΔH_{int} because they best model the interior of the fibril core.

The ΔH_{int} values calculated from the MD simulated Q10 structures are shown in Table 1. Overall, these calculated ΔH_{int} values from the MD simulations are in excellent agreement with our experimentally determined values. We calculate an average ΔH_{int} value of $-6.20(\pm0.63)$ kcal mol^{-1} for side chain−side chain interactions and $-4.30(\pm0.67)$ kcal mol^{-1} for backbone−backbone interactions for the Q10 fibril model. For both the PPII-like and the collapsed β-strand-like monomer structures, we determine that the ΔH_{int} of side chain carbonyl−water interactions is $-4.4(\pm0.61)$ kcal mol^{-1}. For the β-strand-like monomer structure, we calculate that the ΔH_{int} of side chain−backbone hydrogen bonding is $-4.70(\pm0.57)$ kcal mol^{-1}, while that of side chain−side chain hydrogen bonding is $-4.63(\pm0.53)$ kcal mol^{-1}.

Our experimental and computational results indicate that the ΔH_{int} values of side chain−side chain and side chain−backbone interactions of Q10 fibril and monomeric β-strand-like structures are enthalpically more favorable than side chain−water. Interestingly, our results also indicate that in polyQ fibrils side chain−side chain interactions are more favorable than backbone−backbone interactions. The importance of this work is that, to our knowledge, these are the first results that experimentally quantify the relative enthalpic favorability of hydrogen bonding interactions in solution-state and fibril polyQ peptides. This work further validates the hypothesis that interamide side chain and backbone interactions play important roles in thermodynamically driving polyQ-rich proteins toward fibril structures.

COMPUTATIONAL DETAILS

MD simulations were performed using the NAMD software,[47] and VMD was used for visualization and analysis. All simulations were conducted under constant atom number, pressure (1 atm), and temperature (300 K) (*NPT*). The CHARMM36[48] force field was utilized for potential energy and force calculations. The initial coordinates of the simulated structures shown in Figure 2 were from our previously published, experimentally validated work.[34,37] Each system was solvated in TIP3P water.[49] The simulated model fibril system, including water, consisted of a total of 20 284 atoms. The simulations for monomeric PPII-like and β-strand-like Q10 structures with explicit water each consisted of 17 189 atoms. Each system was simulated for 5 ns, and 500 snapshots were extracted from the simulations for analysis. The initial coordinates of each simulated structure, as well as the scripts used in our analysis, are provided in the Supporting Information.

ASSOCIATED CONTENT

Supporting Information

The Supporting Information is available free of charge on the ACS Publications website at DOI: 10.1021/acs.jpclett.8b00348.

Fitting of AmI^S UVRR spectra of Q10 fibrils, estimation of error for determining ΔH_{int} values (PDF)

Coordinate file of the collapsed β-strand Q10 structure simulated via MD (PDB)

Coordinate file of the PPII Q10 structure simulated via MD (PDB)

Coordinate file of fibril Q10 structure simulated via MD (PDB)

AUTHOR INFORMATION

Corresponding Author

*E-mail: asher@pitt.edu.

ORCID

Ryan S. Jakubek: 0000-0001-7880-9422

Sanford A. Asher: 0000-0003-1061-8747

Author Contributions

D.P. and R.S.J. contributed equally to this work.

Notes

The authors declare no competing financial interest.

ACKNOWLEDGMENTS

Funding for this work was provided by the University of Pittsburgh (D.P., R.S.J., S.A.A.), the Defense Threat Reduction Agency HDTRA1-09-14-FRCWMD (R.S.J., S.A.A.), and NIH R01 DA027806 (R.J.W.). MD simulation computer time was supported by XSEDE MCB060069, and computer equipment was purchased from NSF funds (CHE-1126465 and P116Z080180). We thank the late Prof. Jeffry Madura (Duquesne University, Department of Chemistry and Biochemistry) for useful discussions. Also, we thank Stephen White (University of Pittsburgh, Molecular Biophysics and Structural Biology Program), Tim Coleman (University of Pittsburgh, Department of Statistics), and Prof. Satish Iyengar (University of Pittsburgh, Department of Statistics) for assistance in our error estimation.

REFERENCES

(1) Orr, H. T.; Zoghbi, H. Y. Trinucleotide Repeat Disorders. *Annu. Rev. Neurosci.* **2007**, *30*, 575−621.

(2) Chen, S.; Berthelier, V.; Yang, W.; Wetzel, R. Polyglutamine Aggregation Behavior in Vitro Supports a Recruitment Mechanism of Cytotoxicity. *J. Mol. Biol.* **2001**, *311* (1), 173−182.

(3) Mangiarini, L.; Sathasivam, K.; Seller, M.; Cozens, B.; Harper, A.; Hetherington, C.; Lawton, M.; Trottier, Y.; Lehrach, H.; Davies, S. W.; et al. Exon 1 of the HD Gene with an Expanded CAG Repeat Is Sufficient to Cause a Progressive Neurological Phenotype in Transgenic Mice. *Cell* **1996**, *87* (3), 493−506.

(4) Scherzinger, E.; Lurz, R.; Turmaine, M.; Mangiarini, L.; Hollenbach, B.; Hasenbank, R.; Bates, G. P.; Davies, S. W.; Lehrach, H.; Wanker, E. E. Huntingtin-Encoded Polyglutamine Expansions Form Amyloid-like Protein Aggregates in Vitro and in Vivo. *Cell* **1997**, *90* (3), 549−558.

(5) Altschuler, E. L.; Hud, N. V.; Mazrimas, J. a.; Rupp, B. Random Coil Conformation for Extended Polyglutamine Stretches in Aqueous Soluble Monomeric Peptides. *J. Pept. Res.* **1997**, *50* (1), 73−75.

(6) Chen, S.; Berthelier, V.; Hamilton, J. B.; O'Nuallai, B.; Wetzel, R. Amyloid-like Features of Polyglutamine Aggregates and Their Assembly Kinetics. *Biochemistry* **2002**, *41* (23), 7391−7399.

DOI: 10.1021/acs.jpclett.8b00348
J. Phys. Chem. Lett. 2018, 9, 1944−1950

(7) Chellgren, B. W.; Miller, A.-F.; Creamer, T. P. Evidence for Polyproline II Helical Structure in Short Polyglutamine Tracts. *J. Mol. Biol.* **2006**, *361* (2), 362−371.
(8) Klein, F. a C.; Pastore, A.; Masino, L.; Zeder-Lutz, G.; Nierengarten, H.; Oulad-Abdelghani, M.; Altschuh, D.; Mandel, J.-L.; Trottier, Y. Pathogenic and Non-Pathogenic Polyglutamine Tracts Have Similar Structural Properties: Towards a Length-Dependent Toxicity Gradient. *J. Mol. Biol.* **2007**, *371* (1), 235−244.
(9) Wetzel, R. Physical Chemistry of Polyglutamine: Intriguing Tales of a Monotonous Sequence. *J. Mol. Biol.* **2012**, *421* (4−5), 466−490.
(10) Walters, R. H.; Murphy, R. M. Examining Polyglutamine Peptide Length: A Connection between Collapsed Conformations and Increased Aggregation. *J. Mol. Biol.* **2009**, *393* (4), 978−992.
(11) Wang, X.; Vitalis, A.; Wyczalkowski, M. A.; Pappu, R. V. Characterizing the Conformational Ensemble of Monomeric Polyglutamine. *Proteins: Struct., Funct., Genet.* **2006**, *63* (2), 297−311.
(12) Vitalis, A.; Wang, X.; Pappu, R. V. Atomistic Simulations of the Effects of Polyglutamine Chain Length and Solvent Quality on Conformational Equilibria and Spontaneous Homodimerization. *J. Mol. Biol.* **2008**, *384* (1), 279−297.
(13) Vitalis, A.; Lyle, N.; Pappu, R. V. Thermodynamics of Beta-Sheet Formation in Polyglutamine. *Biophys. J.* **2009**, *97* (1), 303−311.
(14) Nakano, M.; Watanabe, H.; Rothstein, S. M.; Tanaka, S. Comparative Characterization of Short Monomeric Polyglutamine Peptides by Replica Exchange Molecular Dynamics Simulation. *J. Phys. Chem. B* **2010**, *114* (20), 7056−7061.
(15) Rhys, N. H.; Soper, A. K.; Dougan, L. The Hydrogen-Bonding Ability of the Amino Acid Glutamine Revealed by Neutron Diffraction Experiments. *J. Phys. Chem. B* **2012**, *116* (45), 13308−13319.
(16) Natalello, A.; Frana, A. M.; Relini, A.; Apicella, A.; Invernizzi, G.; Casari, C.; Gliozzi, A.; Doglia, S. M.; Tortora, P.; Regonesi, M. E. A Major Role for Side-Chain Polyglutamine Hydrogen Bonding in Irreversible Ataxin-3 Aggregation. *PLoS One* **2011**, *6* (4), e18789.
(17) Deng, H.; Callender, R. Enzyme Kinetics and Mechanism Part E: Energetics of Enzyme Catalysis. *Methods Enzymol.* **1999**, *308*, 176−201.
(18) Badger, R. M.; Bauer, S. H. Spectroscopic Studies of the Hydrogen Bond. II. The Shift of the O−H Vibrational Frequency in the Formation of the Hydrogen Bond. *J. Chem. Phys.* **1937**, *5* (11), 839−851.
(19) Levinson, N. M.; Fried, S. D.; Boxer, S. G. Solvent-Induced Infrared Frequency Shifts in Aromatic Nitriles Are Quantitatively Described by the Vibrational Stark Effect. *J. Phys. Chem. B* **2012**, *116* (35), 10470−10476.
(20) Schneider, S. H.; Kratochvil, H. T.; Zanni, M. T.; Boxer, S. G. Solvent-Independent Anharmonicity for Carbonyl Oscillators. *J. Phys. Chem. B* **2017**, *121* (10), 2331−2338.
(21) Choi, J.-H.; Oh, K.-I.; Lee, H.; Lee, C.; Cho, M. Nitrile and Thiocyanate IR Probes: Quantum Chemistry Calculation Studies and Multivariate Least-Square Fitting Analysis. *J. Chem. Phys.* **2008**, *128* (13), 134506.
(22) Pazos, I. M.; Ghosh, A.; Tucker, M. J.; Gai, F. Ester Carbonyl Vibration as a Sensitive Probe of Protein Local Electric Field. Angew. *Angew. Chem.* **2014**, *126* (24), 6194−6198.
(23) Punihaole, D.; Hong, Z.; Jakubek, R. S.; Dahlburg, E. M.; Geib, S.; Asher, S. A. Glutamine and Asparagine Side Chain Hyperconjugation-Induced Structurally Sensitive Vibrations. *J. Phys. Chem. B* **2015**, *119* (41), 13039−13051.
(24) Punihaole, D.; Jakubek, R. S.; Dahlburg, E. M.; Hong, Z.; Myshakina, N. S.; Geib, S.; Asher, S. A. UV Resonance Raman Investigation of the Aqueous Solvation Dependence of Primary Amide Vibrations. *J. Phys. Chem. B* **2015**, *119* (10), 3931−3939.
(25) Mayne, L. C.; Hudson, B. Resonance Raman Spectroscopy of N-Methylacetamide: Overtones and Combinations of the Carbon-Nitrogen Stretch (Amide II′) and Effect of Solvation on the Carbon-Oxygen Double-Bond Stretch (Amide I) Intensity. *J. Phys. Chem.* **1991**, *95* (8), 2962−2967.
(26) Myshakina, N. S.; Ahmed, Z.; Asher, S. a. Dependence of Amide Vibrations on Hydrogen Bonding. *J. Phys. Chem. B* **2008**, *112* (38), 11873−11877.
(27) Wang, Y.; Purrello, R.; Georgiou, S.; Spiro, T. G. UVRR Spectroscopy of the Peptide Bond. 2. Carbonyl H-Bond Effects on the Ground- and Excited-State Structures of N-Methylacetamide. *J. Am. Chem. Soc.* **1991**, *113* (17), 6368−6377.
(28) Markham, L. M.; Hudson, B. S. Ab Initio Analysis of the Effects of Aqueous Solvation on the Resonance Raman Intensities of N-Methylacetamide. *J. Phys. Chem.* **1996**, *100* (7), 2731−2737.
(29) Hudson, B. S.; Markham, L. M. Resonance Raman Spectroscopy as a Test of Ab Initio Methods for the Computation of Molecular Potential Energy Surfaces. *J. Raman Spectrosc.* **1998**, *29* (6), 489−500.
(30) Riddle, F. L., Jr; Fowkes, F. M. Spectral Shifts in Acid-Base Chemistry. 1. van Der Waals Contributions to Acceptor Numbers. *J. Am. Chem. Soc.* **1990**, *112* (9), 3259−3264.
(31) Varfolomeev, M. A.; Rakipov, I. T.; Solomonov, B. N. Calorimetric Investigation of Hydrogen Bonding of Formamide and Its Methyl Derivatives in Organic Solvents and Water. *Int. J. Thermophys.* **2013**, *34* (4), 710−724.
(32) Cutmore, E. A.; Hallam, H. E. Molecular Configuration and Interactions of the Amide group-I: Solvent Effects on Vibrational Frequencies. *Spectrochim. Acta Part A Mol. Spectrosc.* **1969**, *25* (11), 1767−1784.
(33) Eaton, G.; Symons, M. C. R.; Rastogi, P. P. Spectroscopic Studies of the Solvation of Amides with N-H Groups. Part 1.-The Carbonyl Group. *J. Chem. Soc., Faraday Trans. 1* **1989**, *85* (10), 3257−3271.
(34) Punihaole, D.; Jakubek, R. S.; Workman, R. J.; Marbella, L. E.; Campbell, P.; Madura, J. D.; Asher, S. A. Monomeric Polyglutamine Structures That Evolve into Fibrils. *J. Phys. Chem. B* **2017**, *121*, 5953.
(35) Mayer, U.; Gutmann, V.; Gerger, W. The Acceptor Number-a Quantitative Empirical Parameter for the Electrophilic Properties of Solvents. *Monatsh. Chem.* **1975**, *106* (6), 1235−1257.
(36) Chen, S.; Wetzel, R. Solubilization and Disaggregation of Polyglutamine Peptides. *Protein Sci.* **2001**, *10* (4), 887−891.
(37) Punihaole, D.; Workman, R. J.; Hong, Z.; Madura, J. D.; Asher, S. A. Polyglutamine Fibrils: New Insights into Antiparallel β-Sheet Conformational Preference and Side Chain Structure. *J. Phys. Chem. B* **2016**, *120* (12), 3012−3026.
(38) Thakur, A. K.; Jayaraman, M.; Mishra, R.; Thakur, M.; Chellgren, V. M.; L Byeon, I.-J.; Anjum, D. H.; Kodali, R.; Creamer, T. P.; Conway, J. F.; M Gronenborn, A.; Wetzel, R. Polyglutamine Disruption of the Huntingtin Exon 1 N Terminus Triggers a Complex Aggregation Mechanism. *Nat. Struct. Mol. Biol.* **2009**, *16* (4), 380−389.
(39) Sivanandam, V. N.; Jayaraman, M.; Hoop, C. L.; Kodali, R.; Wetzel, R.; van der Wel, P. C. A. The Aggregation-Enhancing Huntingtin N-Terminus Is Helical in Amyloid Fibrils. *J. Am. Chem. Soc.* **2011**, *133* (12), 4558−4566.
(40) Moore, W. H.; Krimm, S. Transition Dipole Coupling in Amide I Modes of β-polypeptides. *Proc. Natl. Acad. Sci. U. S. A.* **1975**, *72* (12), 4933−4935.
(41) Moore, W. H.; Krimm, S. Vibrational Analysis of Peptides, Polypeptides, and Proteins. *Biopolymers* **1976**, *15* (12), 2439−2464.
(42) Moore, W. H.; Krimm, S. Vibrational Analysis of Peptides, Polypeptides, and Proteins. II. β-Poly (L-Alanine) and β-Poly (L-Alanylglycine). *Biopolymers* **1976**, *15* (12), 2465−2483.
(43) Miyazawa, T. Perturbation Treatment of the Characteristic Vibrations of Polypeptide Chains in Various Configurations. *J. Chem. Phys.* **1960**, *32* (6), 1647−1652.
(44) Klotz, I. M.; Franzen, J. S. Hydrogen Bonds between Model Peptide Groups in Solution. *J. Am. Chem. Soc.* **1962**, *84* (18), 3461−3466.
(45) Davies, M.; Thomas, D. K. Energies And Entropies Of Association For Amides In Benzene Solutions. Part II. *J. Phys. Chem.* **1956**, *60* (6), 767−770.
(46) Spencer, J. N.; Garrett, R. C.; Mayer, F. J.; Merkle, J. E.; Powell, C. R.; Tran, M. T.; Berger, S. K. Amide Hydrogen Bonding in Organic Medium. *Can. J. Chem.* **1980**, *58* (13), 1372−1375.

DOI: 10.1021/acs.jpclett.8b00348
J. Phys. Chem. Lett. 2018, 9, 1944−1950

(47) Phillips, J. C.; Braun, R.; Wang, W.; Gumbart, J.; Tajkhorshid, E.; Villa, E.; Chipot, C.; Skeel, R. D.; Kale, L.; Schulten, K. Scalable Molecular Dynamics with NAMD. *J. Comput. Chem.* **2005**, *26* (16), 1781−1802.
(48) Huang, J.; MacKerell, A. D. CHARMM36 All-Atom Additive Protein Force Field: Validation Based on Comparison to NMR Data. *J. Comput. Chem.* **2013**, *34* (25), 2135−2145.
(49) Jorgensen, W. L.; Chandrasekhar, J.; Madura, J. D.; Impey, R. W.; Klein, M. L. Comparison of Simple Potential Functions for Simulating Liquid Water. *J. Chem. Phys.* **1983**, *79* (2), 926−935.

DOI: 10.1021/acs.jpclett.8b00348
J. Phys. Chem. Lett. 2018, 9, 1944−1950